Three-Dimensional Linkage Element Model for Simulation of Failure Behavior of Brittle Materials

George E. VULPE* and Tatsuya TSUBAKI**

* M.S., Graduate Student, Dept. of Civil Engineering, Yokohama National University, Hodogaya-ku, Yokohama 240-8501
** Ph.D., Professor, Dept. of Civil Engineering, Yokohama National University

A three-dimensional simulation model based on the discontinuum modeling method is necessary in order to analyze brittle materials in general stress states more accurately. In this study the linkage element model is used for numerical simulation of the failure behavior of concrete and the damage estimation. The advantage of this approach in the failure simulation of brittle materials is that the internal failure mechanism is clarified by the deformation and the internal mechanical state of each element. Numerical simulation is done to analyze the three-dimensional failure behavior of concrete subject to uniaxial compression.

Key Words : *Discontinuum mechanical model, linkage element, 3D model, concrete, damage, failure*

1. Introduction

There are two main approaches on the failure simulation of concrete: the continuum modeling represented by the finite element method (FEM) and the discontinuum modeling such as the distinct element method (DEM). The FEM is widely implemented in the analysis of concrete structures, but its inherent nature makes it difficult to model cracking behavior of concrete. On the other hand, the discontinuum modeling method can properly model cracking and failure of brittle materials such as concrete. For example, the lattice model was introduced by Schlangen et al.[1] while 2D interface element model was developed by Tsubaki[2] and Abdeen et al.[3] In order to properly analyze the multiaxial state of stress and deformation it is necessary to employ a three-dimensional model. Therefore, a three-dimensional discontinuum mechanical model using linkage elements with an interface in an element is developed in this work and is applied to the analysis of the failure behavior of concrete. The present modeling is aiming at the development of an analysis tool for unreinforced brittle materials of the standard specimen size.

2. Three-Dimensional Linkage Element Model

For the three-dimensional analysis of the failure of brittle materials a 3D linkage element model (LEM) is developed. Concrete is modeled as an assembly of linkage elements with two nodes. Linkage elements with sufficiently small size are used to model the structure of the brittle material.

Two connecting bars are assumed to model the behavior in the normal and tangential directions to the interface which is perpendicular to the line connecting the two nodes. Each connecting bar of a linkage element has a cylindrical shape and length equal to the distance between the two nodes. It is modeled by independent translational and rotational springs whose properties are gradually reduced in order to model material degradation.

At each iteration the system is assumed to behave elastically. The global element stiffness equation is represented as follows:

$$\mathbf{K}^e\,\mathbf{U}^e = \mathbf{F}^e\ ;\ \mathbf{U}^e = \{\mathbf{U}^i,\mathbf{U}^j\}^T\ ;\ \mathbf{F}^e = \{\mathbf{F}^i,\mathbf{F}^j\}^T \quad (1)$$

where $\mathbf{K}^e$ is the global element secant stiffness matrix and $\mathbf{F}^e$ is the global element nodal forces corresponding to the global element nodal displacements $\mathbf{U}^e$. Displacements and forces at node *i* are represented by generalized displacement vector $\mathbf{U}^i$ and force vector $\mathbf{F}^i$:

$$\mathbf{U}^i = \{\, u^i_x, u^i_y, u^i_z, \theta^i_x, \theta^i_y, \theta^i_z \,\}^T \quad (2)$$

$$\mathbf{F}^i = \{\, f^i_x, f^i_y, f^i_z, m^i_x, m^i_y, m^i_z \,\}^T \quad (3)$$

where u^i_x, u^i_y, u^i_z are the global displacement components, θ^i_x, θ^i_y, θ^i_z are the global rotation angles, f^i_x, f^i_y, f^i_z are the resultant forces at node *i*, and m^i_x, m^i_y, m^i_z are the resultant moments. The relative normal and tangential displacements and rotation angles can be expressed in terms of displacements at nodes *i* and *j*:

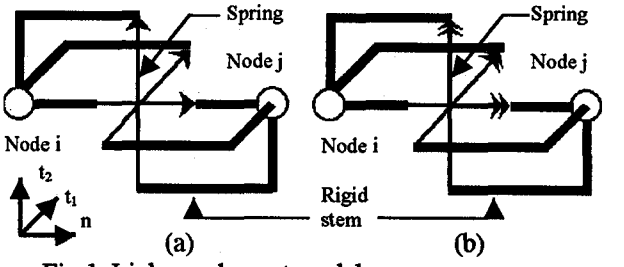

Fig.1 Linkage element model:
(a) translational springs, (b) rotational springs

$$\mathbf{V}^e = \mathbf{T}^e(\mathbf{U}^j - \mathbf{U}^i) \quad (4)$$

$$\mathbf{V}^e = \{ v^e_n , v^e_{t1} , v^e_{t2} , \omega^e_n, \omega^e_{t1} , \omega^e_{t2} \}^T \quad (5)$$

where $\mathbf{T}^e$ is a 6x6 ordinary three-dimensional coordinate transformation matrix from the global coordinate system x, y, z to the local coordinate system n, t_1, t_2. The normal and tangential force components and moments in the local coordinate system are:

$$\mathbf{F}^e = \{ f^e_n , f^e_{t1} , f^e_{t2} , m^e_n , m^e_{t1} , m^e_{t2} \}^T \quad (6)$$

The linkage element is characterized by the following local force - relative displacement relationship:

$$\mathbf{F}^e = \mathbf{k}^e \mathbf{V}^e \quad (7)$$

$$\mathbf{k}^e = \begin{bmatrix} \mathbf{k}^f & \mathbf{0} \\ \mathbf{0} & \mathbf{k}^m \end{bmatrix} \quad (8)$$

$$\mathbf{k}^f = \begin{bmatrix} k^f_n & 0 & 0 \\ 0 & k^f_{t1} & 0 \\ 0 & 0 & k^f_{t2} \end{bmatrix}; \mathbf{k}^m = \begin{bmatrix} k^m_n & 0 & 0 \\ 0 & k^m_{t1} & 0 \\ 0 & 0 & k^m_{t2} \end{bmatrix} \quad (9)$$

where $\mathbf{k}^e$ represents the stiffness of the material. k_n^f is for the normal spring, k_{t1}^f, k_{t2}^f are for the tangential springs, k_n^m is for the torsional spring, and k_{t1}^m, k_{t2}^m are for other rotational springs.

3. Material Modeling

3.1 Stress-Strain Relationship

The stress-strain relationship for a brittle material is assumed linear elastic up to the peak. The maximum stress failure criterion is used and it is examined independently in normal and tangential directions. The element must be checked for the normal translation, two tangential orthogonal translations and rotation around each axis (accounting for torsional and flexural components). Failure is assumed to be brittle in tension and ductile in compression and shear. Figure 2 shows the stress-strain diagrams in the normal and tangential directions in order to model the behavior of a brittle material such as concrete.

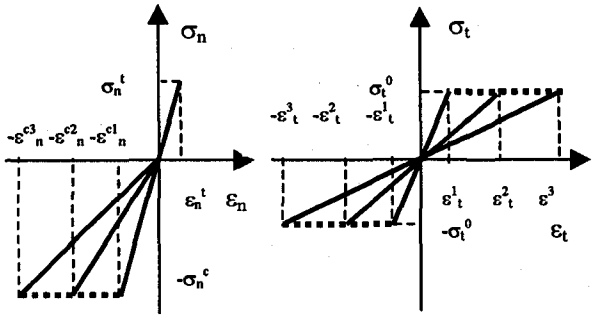

(a) (b)

Fig.2 Schematic stress-strain diagram for material of linkage element: (a) normal direction, (b) tangential direction

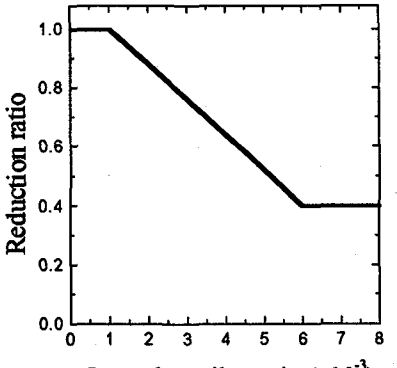

Fig.3 Reduction of compressive strength as a function of lateral tensile strain

3.2 Failure Criteria

The gradual degradation model is assumed in shear and compression by reducing the stiffness each time the failure condition is satisfied at one linkage element layer. Failure is determined by the maximum stress failure criterion. A compressive strength reduction law takes into account the material strength degradation due to lateral tensile strain. The lateral strain dependence of compressive strength is shown in Fig.3. This reduction law accounts for the effect of tensile cracking and formation of continuous cracks in early stages.

3.3 Gradual Degradation Model

In compression and shear, the stepwise reduction of the stiffness is employed each time the failure criterion is satisfied. The reduction rate used in case of compression, shear and tension failure are shown in Fig. 4.

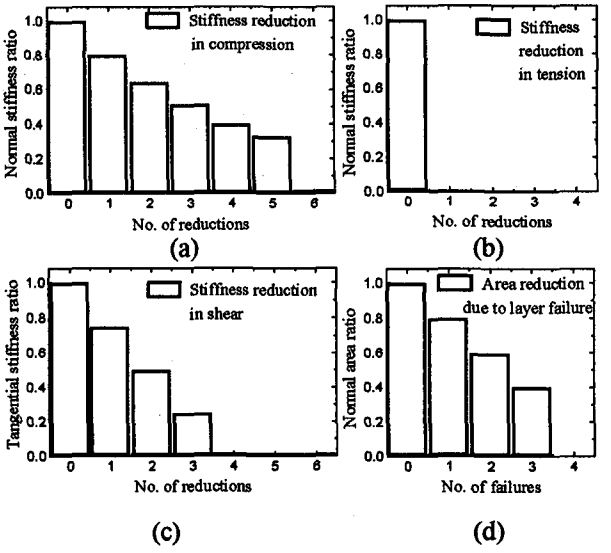

Fig.4 Reduction of element stiffness and area: (a) compressive, (b) tensile, (c) shear stiffness and (d) area

3.4 Linkage Element Model

The connecting bar of the linkage element has a cylindrical shape and is divided into concentric layers with equal area. The stresses are determined at the most external layer where stresses take the maximum value. The layers account for the gradual degradation of the sectional characteristics. The most external layer is removed every time the failure criterion is satisfied but the section remains circular. The connecting bar is

assumed to fail when 60% of the layers failed. Figure 4 (d) shows the reduction of area of the element due to failure of layers.

The initial cross-sectional area of the element is determined at the start of the simulation, is a function of its length and is assumed not to vary unless failure occurs. The areas of the normal and tangential connecting bars are considered independently and are equal for elements of the same type. The area of each layer A^l_n, A^l_t is taken to be a fraction of the total area of each connecting bar A_n, A_t.

$$A_n^l = \frac{A_n}{n_l} \qquad A_t^l = \frac{A_t}{n_l} \tag{10}$$

where n_l is the total number of layers.

The stiffness corresponding to the normal spring k_n^f, the tangential springs k_{t1}^f, k_{t2}^f, the rotational springs k_{t1}^m and k_{t2}^m, and the torsional spring k_n^m are calculated as:

$$k_n^f = \frac{E_n A_n}{L_m} \tag{11}$$

$$k_{t1}^f = k_{t2}^f = \frac{G_t A_t}{L_m} \tag{12}$$

$$k_{t1}^m = k_{t2}^m = \frac{\alpha E_n I_n}{L_m} \tag{13}$$

$$k_n^m = \frac{\beta G_t J_t}{L_m} \tag{14}$$

where E_n and G_t are the elastic modulus and shear rigidity of each connecting bar, L_m is the distance between nodes, and α, β are nondimensional proportional constants.

The maximum stresses are determined independently for the normal and tangential connecting bar of the linkage element (see Fig. 5).

$$\sigma_{n,\max} = \frac{f_n^c}{A_n} + \sqrt{\left(\frac{m_{t1}^c R_n}{I_n}\right)^2 + \left(\frac{m_{t2}^c R_n}{I_n}\right)^2} \tag{15}$$

$$\sigma_{t,\max} = \sqrt{\left(\frac{f_{t1}^c}{A_t}\right)^2 + \left(\frac{f_{t2}^c}{A_t}\right)^2} + \frac{m_n^c R_t}{J_t} \tag{16}$$

where R_n, R_t are the radii of each connecting bar, I_n is the moment of inertia and J_t is the torsional constant of each connecting bar.

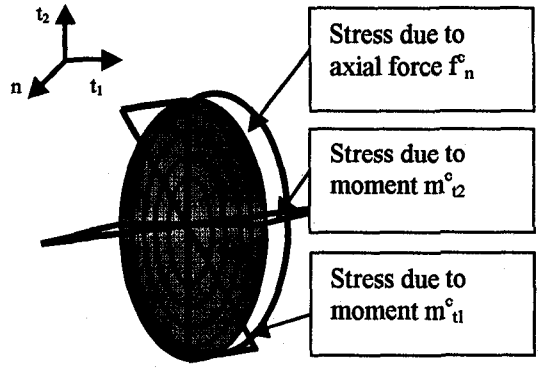

Fig.5 Layers and normal stress distribution in the cross section of connecting bar

4. Computational Algorithm

The analysis procedure is based on the secant analysis method in order to obtain computational stability. It consists in imposing unit displacements or forces and determining nodal displacements from the equilibrium equations. Taking into account the corresponding relative displacements between nodes of each element, stresses for all elements are determined.

Considering the ratio between stresses and strengths at each element, the value of the force that determines failure in only one element is obtained. After the reduction of the corresponding element stiffness, the computational procedure is continued until final failure. At each step the displacements of nodes are determined and the position of the nodes is updated. The flow of the algorithm is shown in Fig.6.

The secant analysis method used in this study is a simple and efficient computational procedure for a monotonic proportional loading which is considered in the following simulation example. From its inherent nature, however, it is difficult to apply to the analysis of a problem for a nonproportional or cyclic loading.

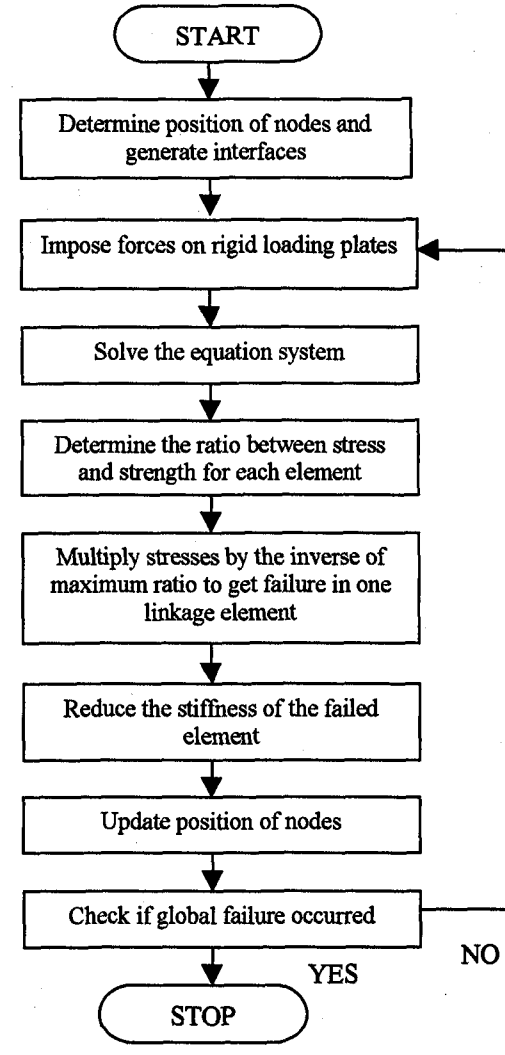

Fig.6 Flow of secant analysis method

5. Simulation Results

A numerical simulation is made for the experimental results by Van Mier[4] on concrete subject to uniaxial compression. The specimen used in Van Mier's experiment is a cube (10x10x10cm) of concrete with compressive strength σ^n_c=45 N/mm^2.

The mesh is chosen so that its global initial behavior gives an isotropic elastic response in the global coordinate directions (see Fig.7). The apparent Poisson's ratio is for this mesh 0.218. This value is close to the typical value for concrete. It consists of nodes arranged into nine planes parallel with the specimen sides. Nodes located into the same plane are connected by horizontal and vertical elements while nodes located in neighboring planes are connected by diagonal elements. In Fig.7 nodes located on the first and third planes are shown in black while intermediate nodes on the second plane are gray.

The present 3D mesh consists of 189 nodes and 956 elements arranged as in Fig.7. The length of vertical and horizontal elements is 2.5cm while that of diagonal elements is 2.165cm. Elements are distributed in the horizontal and vertical axis directions (15.5% on each direction) and in the diagonal direction (53.5%).

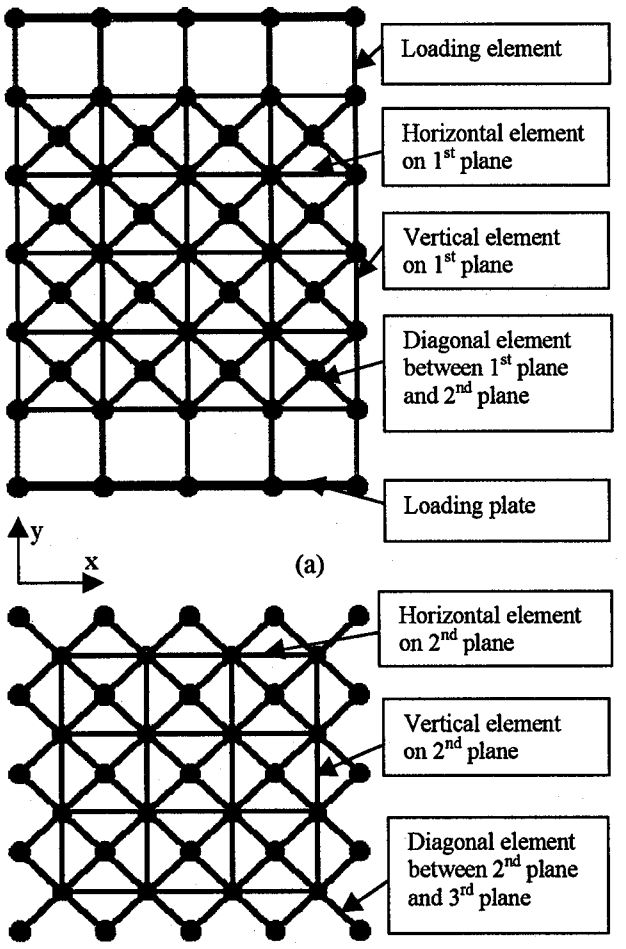

Fig.7 Side view of the mesh used in simulation:
(a) linkage elements in the 1st plane of nodes,
(b) linkage elements in the 2nd plane of nodes

The boundary conditions are given by using special elements. The loading plates are represented by a plane of nodes connected by elements with high rigidity in the transverse direction. The role of the rigid loading plates is to assure the correct loading conditions without additional computational steps. In order to simulate boundary conditions equivalent with the loading brushes used in the experiment, normal elements connect the loading plate with the specimen. The load is applied in the y-direction by uniform load given on the upper loading plate.

The strength is assumed to be the same for all elements. However, the strength of one element of a specimen center is reduced so as cracking to start from a known point and simulation to be reproducible.

In uniaxial compression, after the initial linear elastic behavior, the stress-strain diagram (Fig.8) shows a descending branch modeling the softening. The stress increases gradually up to the peak (obtained after 150 iterations) and then gradually decreases. When a large number of elements already failed the specimen crushes. The stress-strain diagram on x and z directions are shown in Fig. 9. In both x and z directions lateral expansion is observed. Values of strain are slightly different due to nonuniform cracking.

The volumetric expansion due to lateral expansion of the specimen is observed before the peak. In the final stage crushing of the specimen occurs because of the rapid degradation of the stiffness. An increasing number of elements in the mesh will generate a smoother diagram and a slower rate of reduction of the stiffness.

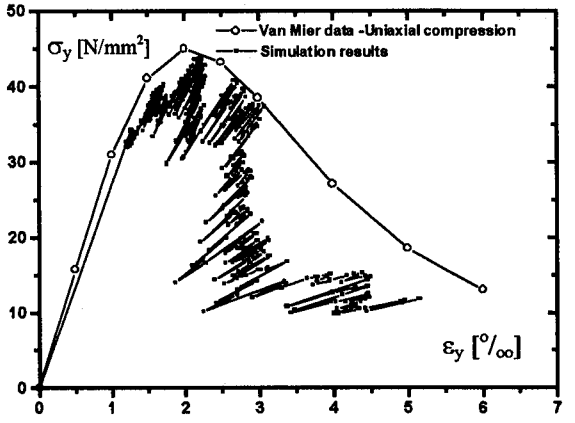

Fig.8 Stress-strain diagram in uniaxial compression

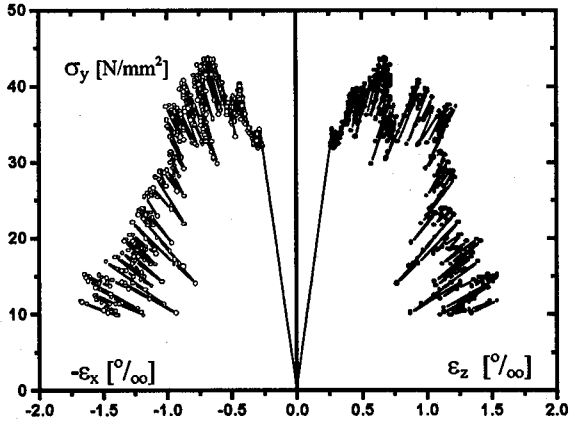

Fig.9 Stress-strain diagram in lateral direction

For this uniaxial compression loading of a cubic concrete specimen the deformation and cracking of the specimen are shown in Figs.10, 11, 12.

In Fig.10 presented is the deformation of the specimen in a central section parallel to xy plane. The deformational behavior of the specimen can be followed at each step. In Fig.10(a-c) the gray circles indicate the initial position of the nodes, black circles indicate displaced position of the nodes while the segments linking the gray circles to the black circles indicate the displacement vector. Displacements are represented by multiplying by a scale factor. Shapes of the original and deformed specimen are plotted with gray and black line respectively. It is observed that the deformation increases significantly after the peak especially in zones where intense cracking process occurs.

The early crack pattern is shown in Figs.11(a) and 12(a). The black lines show failed interfaces due to tension while the circles indicate the position of the nodes. In step 75 which is on the ascending part of the load-displacement curve all cracks are vertical due to lateral tension. At the peak (step 150) most of the failures are due to vertical elements but there are few diagonal elements failed in tension. Later, tensile vertical and diagonal cracks are propagating through the specimen as seen in Figs.11(c) and 12(c) (step 350). In the final stage, shear and compression failures occur leading to the global failure of the specimen.

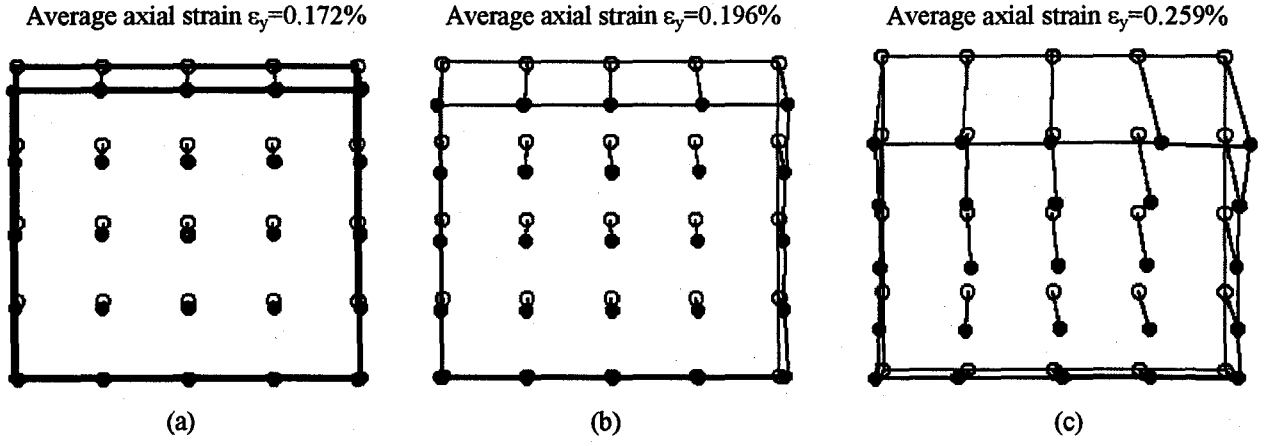

Fig.10 Deformation in a section in xy plane: (a) step 75, (b) step 150 and (c) step 350

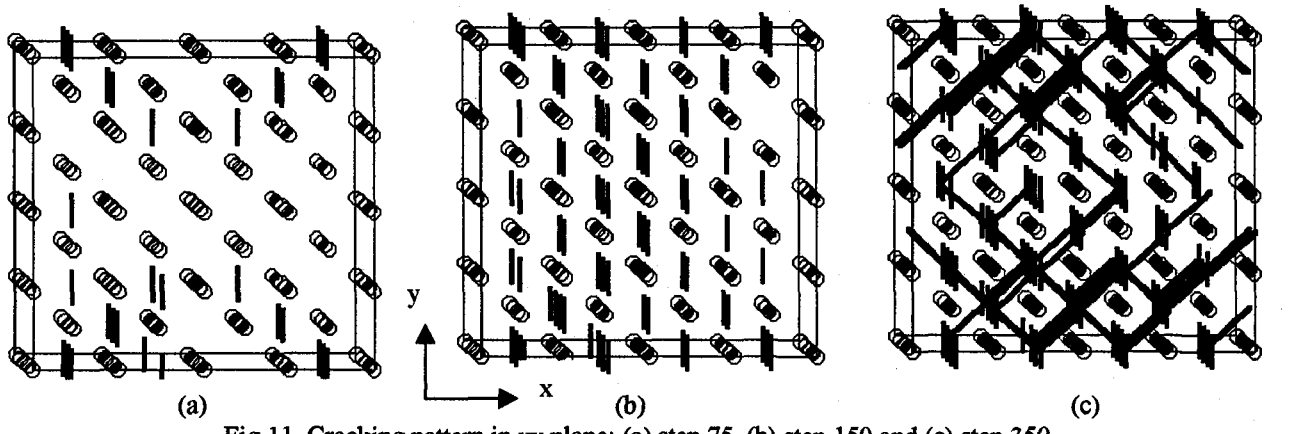

Fig.11 Cracking pattern in xy plane: (a) step 75, (b) step 150 and (c) step 350

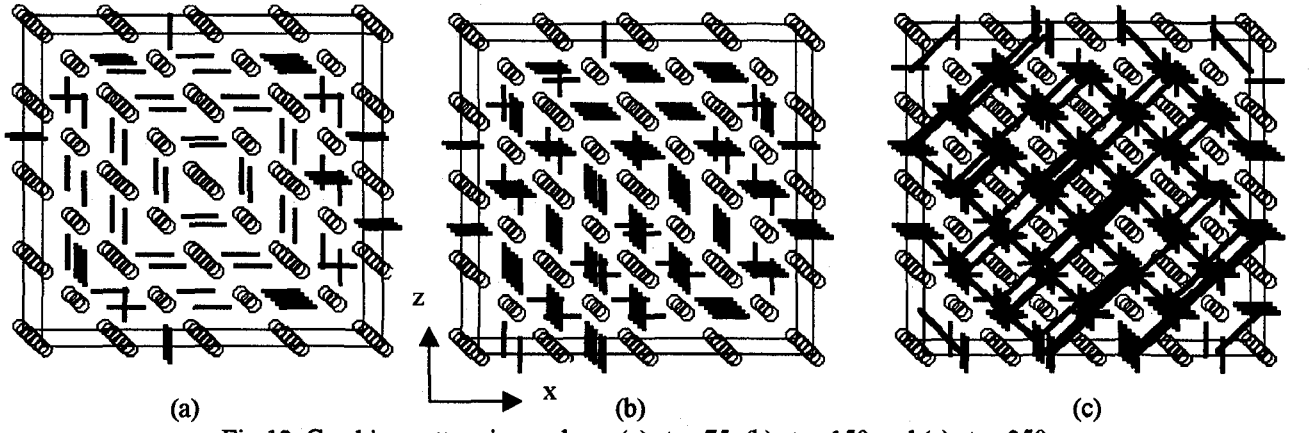

Fig.12 Cracking pattern in zx plane: (a) step 75, (b) step 150 and (c) step 350

Figure 13 shows the distribution of crack and the crack opening projected on the xy plane at steps 150 and 350. The width of the line showing a tensile crack is proportional to the crack opening. It is observed that the cracks are uniform and their width is small in early stage. After 350 steps (see Fig.13 (b)) the cracks are wide opened showing that the material is expanding laterally.

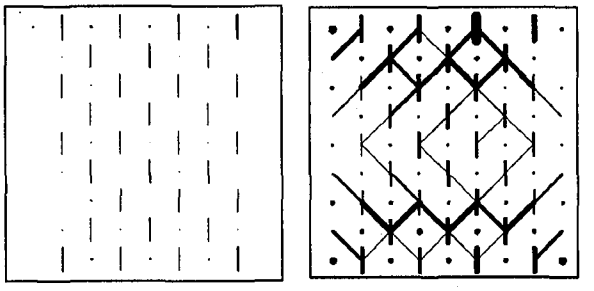

(a) (b)

Fig.13 Opening of crack and crack distribution: (a) step 150, (b) step 350

The damage of the material can be expressed by the evolution of a damage indicator similar to the one proposed by Abdeen et al.[5]. The damage indicator D shows crack development due to tensile failure of horizontal, vertical and diagonal elements and is defined in each direction as follows:

$$D = \sum_{j=1}^{N_{FE}} A(j) \Big/ \sum_{k=1}^{N_E} A(k) \qquad (17)$$

where A(j) stands for the area of element j. This damage indicator gives the ratio between the failed element area and the total element area of the specimen. N_{FE} is the number of elements failed in tension and N_E is the total number of elements in the direction considered. The values of D for linkage elements in each direction failed in tension are shown in Fig.14.

In the early stage only vertical cracks develop and at the peak the value of damage indicator for horizontal element is 0.50. After the peak, some diagonal elements failed and at step 350 the value of D for horizontal directions reaches 0.79 while the value for diagonal direction is 0.15 indicating vertical and diagonal cracking.

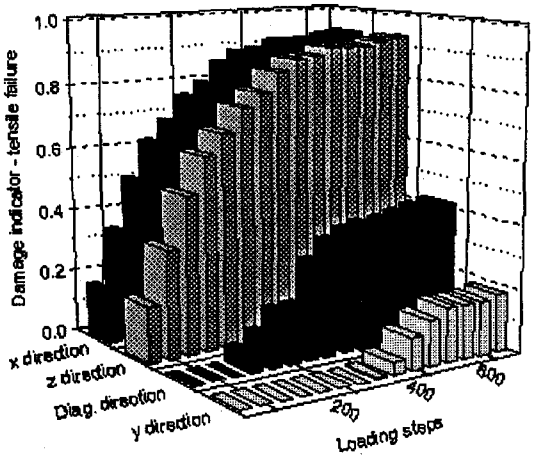

Fig.14 Damage indicator for tensile failure of each direction

6. Conclusions

It is confirmed that the present 3D linkage element model can be used in the failure simulation of a brittle composite material such as concrete. By the present method it is possible to follow the degradation of material and the deformation. Obtained stress-strain diagrams show satisfactory agreement with experimental data. The same mesh can be tested in biaxial and triaxial compression tests under small lateral confinement stress. The model is used to estimate the internal failure mechanism. By including the reinforcement effect, it can be extended to the modeling of structural elements. The major findings are as follows.

1) The overall deformational behavior of a brittle material can be followed in a general stress state.
2) The degradation of the material is observed and can be quantified. The cracking development and the crack opening are obtained for all stages until the final failure occurs.
3) Phenomena such as strain-softening and volumetric expansion are simulated with the present model.

Appendix; Constants Used in Simulation

Elasticity modulus	E_n=32500 N/mm^2
Shear modulus	G_t=13500 N/mm^2
Compressive strength	σ^c_n=45.0N/mm^2
Tensile strength	σ^t_n=4.5 N/mm^2
Shear strength	σ^o_t=4.5 N/mm^2
Normal area of diagonal elements	A_n=14 mm^2
Tangential area of diagonal elements	A_t=1.2 mm^2
Number of layers	n_l=5

Area of diagonal elem. / Area of normal elem. = 2

Proportional constants: $\alpha=4(L_m/R_n)^2$; $\beta=2(L_m/R_t)^2$

References

1) Schlangen, E. and van Mier, J.G.M.: Simple lattice model for numerical simulation of fracture of concrete materials and structures, *Materials and Structures*, No.25, pp.534-542, 1992.
2) Tsubaki, T.: Numerical simulation of deformational properties of concrete using microstructural unit elements, *Trans. of JCI.*, Vol.17, pp.119-126, 1995.
3) Abdeen, A.M.A. and Tsubaki, T.: Disk element model for failure behavior of concrete under biaxial stresses, *Journal of Struct. Eng.*, Vol.42A, pp. 239-246, 1996.
4) Van Mier, J.G.M.: Multiaxial strain-softening of concrete, *Materials and Structures*, Vol.19, No.111, pp.179-190, 1986.
5) Abdeen, A.M.A. and Tsubaki, T.: Simulation of failure behavior of high strength concrete under compression, *Proc. of Cairo 1st Conference on Concrete Structures*, Vol.3, pp.44-55, 1996.

(Received September 18, 1998)